Designing a High-Precision AC Current Source to Measure the nm-Scale Displacements in Mechanical Systems

Lanto Rasolofondraibe, Bernard Pottier, Xavier Chiementin

Hindawi
Journal of Sensors
Volume 2019, Article ID 9451808, 9 pages
https://doi.org/10.1155/2019/9451808

Research Article

Designing a High-Precision AC Current Source to Measure the nm-Scale Displacements in Mechanical Systems

Lanto Rasolofondraibe[1], **Bernard Pottier**[1] and **Xavier Chiementin**[2]

[1]*Laboratory CRESTIC, University of Reims Champagne-Ardenne, Moulin de la Housse, BP 103951089, Cedex 2, Reims, France*
[2]*GRESPI, University of Reims Champagne-Ardenne, Moulin de la Housse, BP 103951089, Cedex 2, Reims, France*

Correspondence should be addressed to Lanto Rasolofondraibe; lanto.rasolofondraibe@univ-reims.fr

Received 14 March 2018; Revised 22 August 2018; Accepted 8 October 2018; Published 11 April 2019

Academic Editor: Paolo Bruschi

Measuring the dynamics of a continuously moving target, at the nanoscale level, such as of a bearing raceway or any other vibrating element, requires a contactless measurement. A mission that can be easily carried out by a capacitive probe. The current flowing through the sensor has to remain constant regardless of the changes in the sensors' output impedance. In this manner, the voltage across the probe is proportional to the distance between the probe and the target. However, the high impedance of the probe cannot be disregarded in comparison to the output impedance of the Howland source. To overcome this problem, we designed a voltage-controlled AC current source (VCCS). The new design consists of implementing two nested loops and uses two cascaded controllers, a fast but imprecise internal control loop tuned by a slow but precise outer control loop in order to obtain a high-precision AC output current. The performance of this device has been compared with the improved quad op-amp current source (IQOA). The results obtained during the numerical validation confirm the relevance of this device.

1. Introduction

A simple and accurate way to measure impedance is to inject a constant alternating current and measure the voltage across it. Howland designed the first op-amp current source in 1964 [1]. Since then, many variations have been designed to enhance it.

(i) Advanced Howland current source
(ii) Mirrored modified Howland current source
(iii) Implemented improved current source
(iv) Dual op-amp current source (DOA)

These current sources have already been studied (see [2–8]).

They are widely used in different fields of applications such as the following:

(1) Medical field
  (a) Electrical impedance tomography (EIT) [9–12]
  (b) Neurostimulation system [13–15]
  (c) Multifrequency electrical bioimpedance (MEB), also called impedance spectroscopy [16–18]

In these medical applications, the AC current source can be used in a wideband frequency (within the range of 10 Hz to 10 MHz) and the bioimpedances are rather small (between 100 Ω and to 1 MΩ) compared to the output impedance of the AC source current (from 1 MΩ up to 50 MΩ).

(2) Mechanical field Measuring the dynamics of a continuously moving target, at the nanometer scale, such of an outer race or any other vibrating element requires a noncontact measurement. The capacitive sensor can easily fulfill this task. The voltage across the capacitor is proportional to the distance between the target and the probe if a constant alternating current is flowing through the probe. These sensors are called "capacitive linear displacement transducer," [19–22].

In these mechanical applications, measurement is more difficult to achieve because of the following:

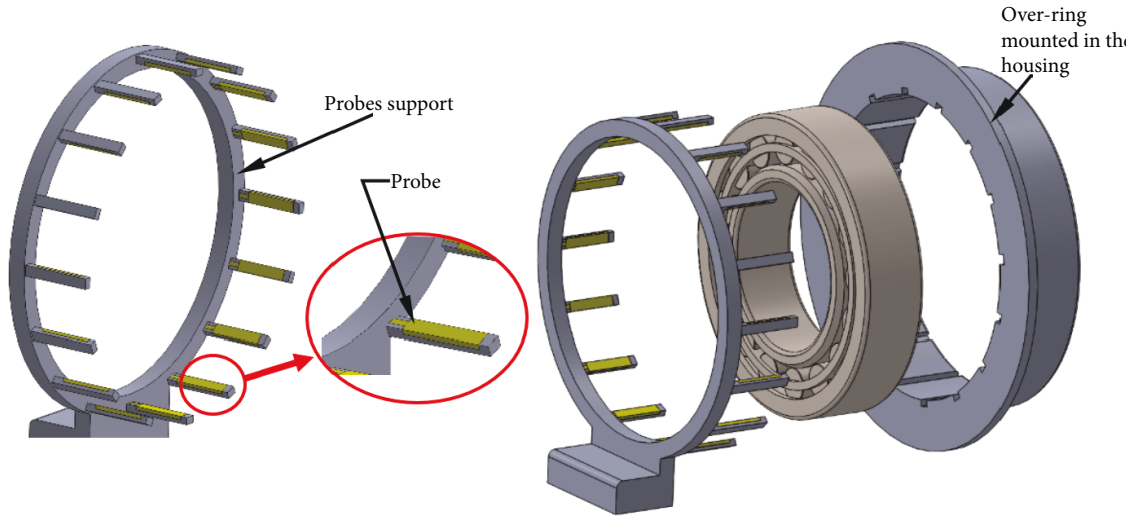

Figure 1: Rolling bearing instrument with capacitive probes.

(i) The high impedances of these sensors are between 150 kΩ and up to 15 MΩ so they can no longer be neglected when compared to the output impedance

(ii) A small change in the gap induces a significant change in the probe's impedance, which may induce a change in the current flowing through the probe

(iii) At last, the bandwidth of the current source should be large enough (between 10 kHz and 100 kHz) to suit all mechanical applications (rolling bearing inside the machine tool, spindle rotating at high speed, disk drive spindles, high-speed drill spindles, vibration measurements, etc.)

A voltage-controlled current source is needed for these mechanical applications [23–29].

In this paper, we briefly describe a rolling bearing equipped with 16 capacitive probes in order to measure its outer ring vibrations' amplitudes and frequencies. Considering the parameters of operational amplifiers, we will first establish an analytical model of the current source. Then, a PSPICE software modelling and simulation software will be carried out to verify the validity of this analytical model. Since the current source has showed to be not efficient enough to measure displacements in the nanometer scale, we designed a voltage-controlled current source that consists of two cascaded controllers, a fast but not precise inner control loop regulated by a slow but precise outer control loop, which will help us obtain a high-precision AC output current that can reach several MHz. Finally, we will present the performances of this device.

2. Displacement Measurement Δd_{avg}

The SKF NU 210 ECP rolling bearing is instrumented with 16 capacitive probes (Figure 1). Numerical simulations with ABAQUS software were carried out to estimate the vibrations' amplitude (Figure 2, Equation (1)) of the bearing raceway [30]:

$$0 \leq \Delta d_{\text{avg}} \leq 3\,\mu\text{m}. \tag{1}$$

Each probe is at a floating voltage and the rolling bearing is connected to the common voltage. The "target area" is the bearing ring's surface located beneath the probe (Figure 3). This surface is decomposed in N elementary areas. The probe capacitance is equal to the sum of all these elementary plane capacitances ([31], Equation (2)).

$$C_{\text{probe}} = \sum_{i=1}^{N} c_i = \varepsilon A_{\text{probe}} \times \frac{1}{D_0 - d_{\text{avg}}} = \frac{\varepsilon A_{\text{probe}}}{D}. \tag{2}$$

d_{avg} is given by the following:

$$d_{\text{avg}} = \frac{\sum_{i=1}^{N} d_{ij}}{N}, \tag{3}$$

where θ is the angular position of the rolling element under the probe; F_r is the radial force transmitted by the rolling element; A_{probe} is the active surface of the probe, which is equal to 5.6 mm^2; $d_{\text{avg,max}} = 3\ \mu$m; D_0 is the initial gap, equal to 0.05 ± 0.01 mm; and D_0 is never the same under each probe.

Then, the probe impedance is given by

$$Z_{\text{probe}}(f, D) = \frac{1}{\varepsilon 2\pi f A_{\text{probe}}} \times D. \tag{4}$$

The probe's voltage amplitude is given by

$$V_{\text{probe}} = Z_{\text{probe}}.I_{\text{probe}} = \frac{I_{\text{probe}}}{2\pi f \varepsilon A_{\text{probe}}} \times D = K_{\text{probe}} \times I_{\text{probe}} \times D. \tag{5}$$

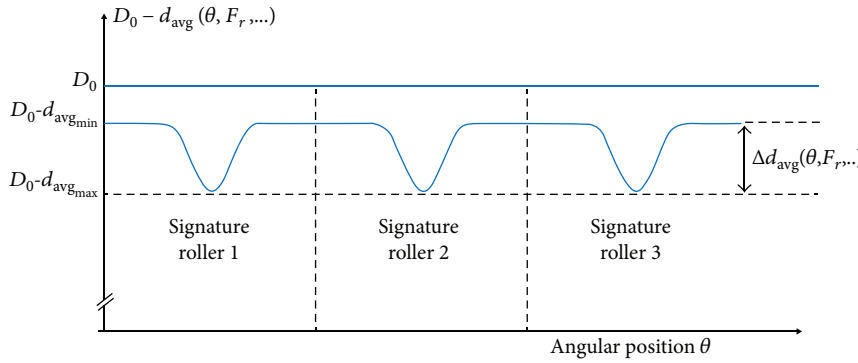

Figure 2: The amplitudes of the vibrations (simulation ABAQUS).

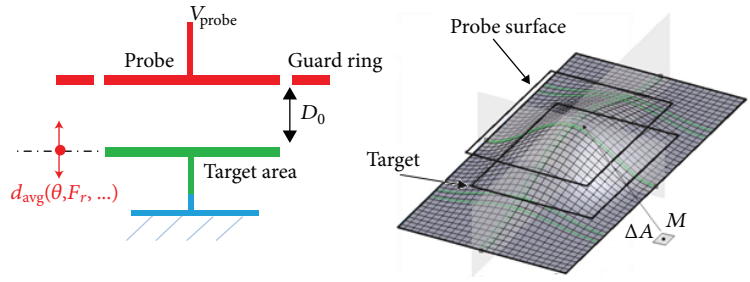

Figure 3: The probe's capacitor.

The parameters remain constant during measurements and can therefore be substituted by a constant: K_{probe}.

When the current remains constant, the probe voltage varies in proportion to the gap. Accordingly, the displacement measurement can be given by

$$\Delta V_{probe} = K_{probe} \times I_{probe} \times \Delta d_{avg},$$
$$\Delta d_{avg} = \frac{\Delta V_{probe}}{K_{probe} \times I_{probe}} = \frac{\Delta V_{probe}}{S_{probe}}. \quad (6)$$

S_{probe} corresponds to the sensitivity of the probe (mV/μm). Moreover, to measure the sixteen displacements with the same accuracy, the current must remain the same through each probe even if impedances are not equal.

3. Modeling an Improved Quad Op-Amp Current Source (IQOA)

This improved quad op-amp current source (IQOA) has the advantage of being easily inserted in a control loop with two inputs (Figure 4). To present a better qualitative description of the used Howland source, we included bode diagrams of $Z_{out}(f)$ and $I_{out}(f)$.

Its equivalent impedance Z_{out} is the impedance obtained at the terminals A–B of the network with the source voltages of V_1 and V_2 short-circuited. Its equivalent current I_{out} is the current obtained at the terminals A–B of the network with terminals A–B short-circuited. We take into account the following op-amp characteristics:

$$a = A_0 \frac{A_0}{1 + j(f/f_0)}, \quad (7)$$

where A_0 is the DC open-loop gain, f_0 is the cutoff frequency, $Z_{in} \longrightarrow \infty$, and $Z_s \longrightarrow 0\ \Omega$.

The output impedance Z_{out} is given by the following (Figure 5):

$$Z_{out}(f) = \left(-\frac{V_{out}}{I_{out}}\right)_{V_{in}=0} = \frac{(a+1)(a+2)}{(3a+2)} \times R_{probe} = A(f) \times R_{probe}. \quad (8)$$

The output current I_{out} is given by the following (Figure 6):

$$I_{out} = \frac{1}{R_{probe}} \times \frac{a^2\left(1 + 2(R_2/R_G)\right)}{(a+2)\left[a + 1 + 2\left(R_2/R_G\right)\right]} \times (V_1 - V_2), \quad (9)$$

when $R_G = 2 \times R_2$,

$$I_{out} = \frac{a^2}{(a+2)(a+2)} \times \frac{2(V_1 - V_2)}{R_{probe}} = B(f) \times \frac{2(V_1 - V_2)}{R_{probe}}. \quad (10)$$

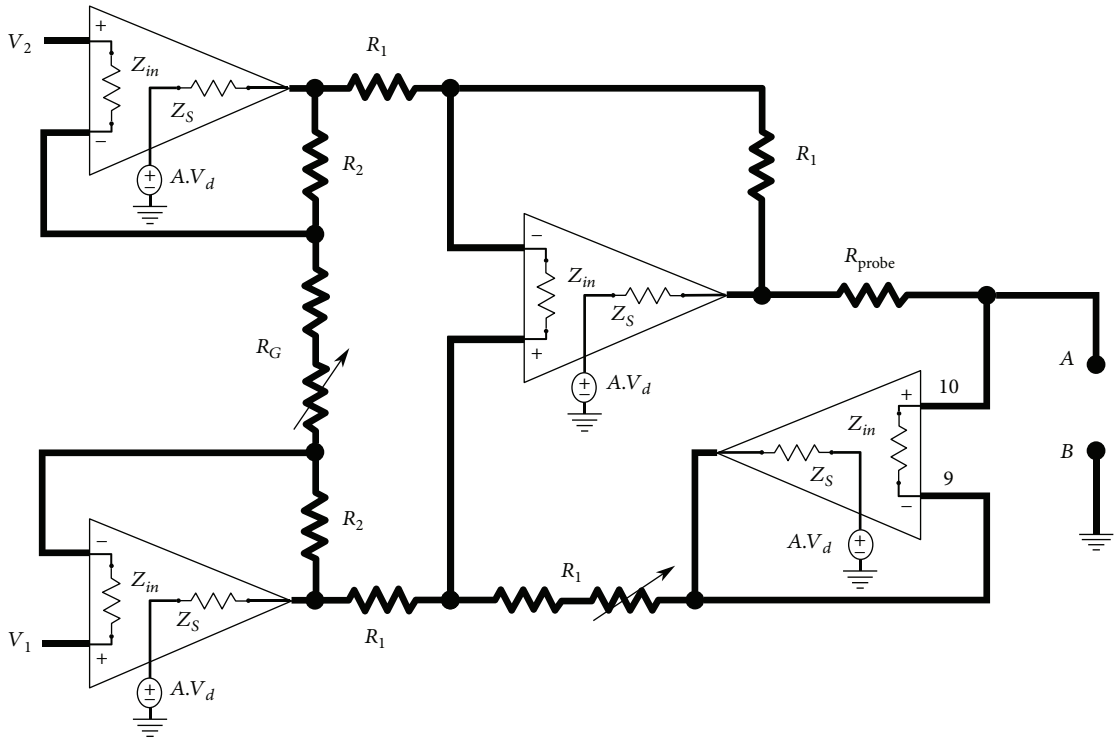

Figure 4: Improved quad op-amp current source (IQOA).

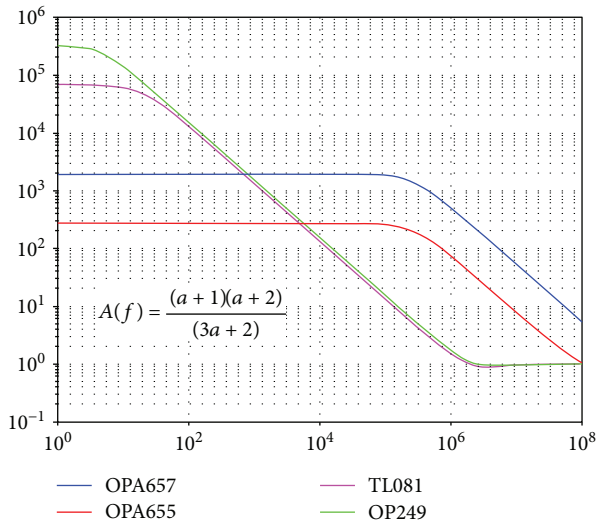

Figure 5: Modelling IQOA $A(f)$.

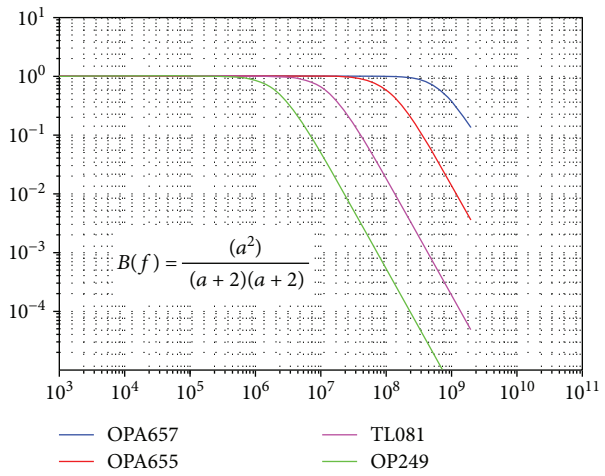

Figure 6: Modelling IQOA $B(f)$.

This analytical model has been validated by PSPICE simulations.

4. Voltage Controlled Current Source (VCCS)

4.1. Insufficient Performances of the Power Source. Our aim is to design an electronic device capable of establishing nanoscale displacement measurements (≈ 10 nm). Nanoscale resolution requires

$$\begin{aligned}
\frac{\Delta\left(\Delta d_{\text{avg}}\right)}{D} &= \frac{\Delta V_{\text{probe}}}{V_{\text{probe}}} + \frac{\Delta I_{\text{probe}}}{I_{\text{probe}}} + \frac{\Delta K_{\text{probe}}}{K_{\text{probe}}},\\
\frac{\Delta\left(\Delta d_{\text{avg}}\right)}{D} &= \frac{10\text{ nm}}{60.10^3\text{ nm}} = 0.018\%,\\
\frac{\Delta V_{\text{probe}}}{V_{\text{probe}}} &= 0.002\%,\\
\frac{\Delta K_{\text{probe}}}{K_{\text{probe}}} = 0 &\Rightarrow \frac{\Delta I_{\text{probe}}}{I_{\text{probe}}}(D) \le 0.016\%.
\end{aligned} \tag{11}$$

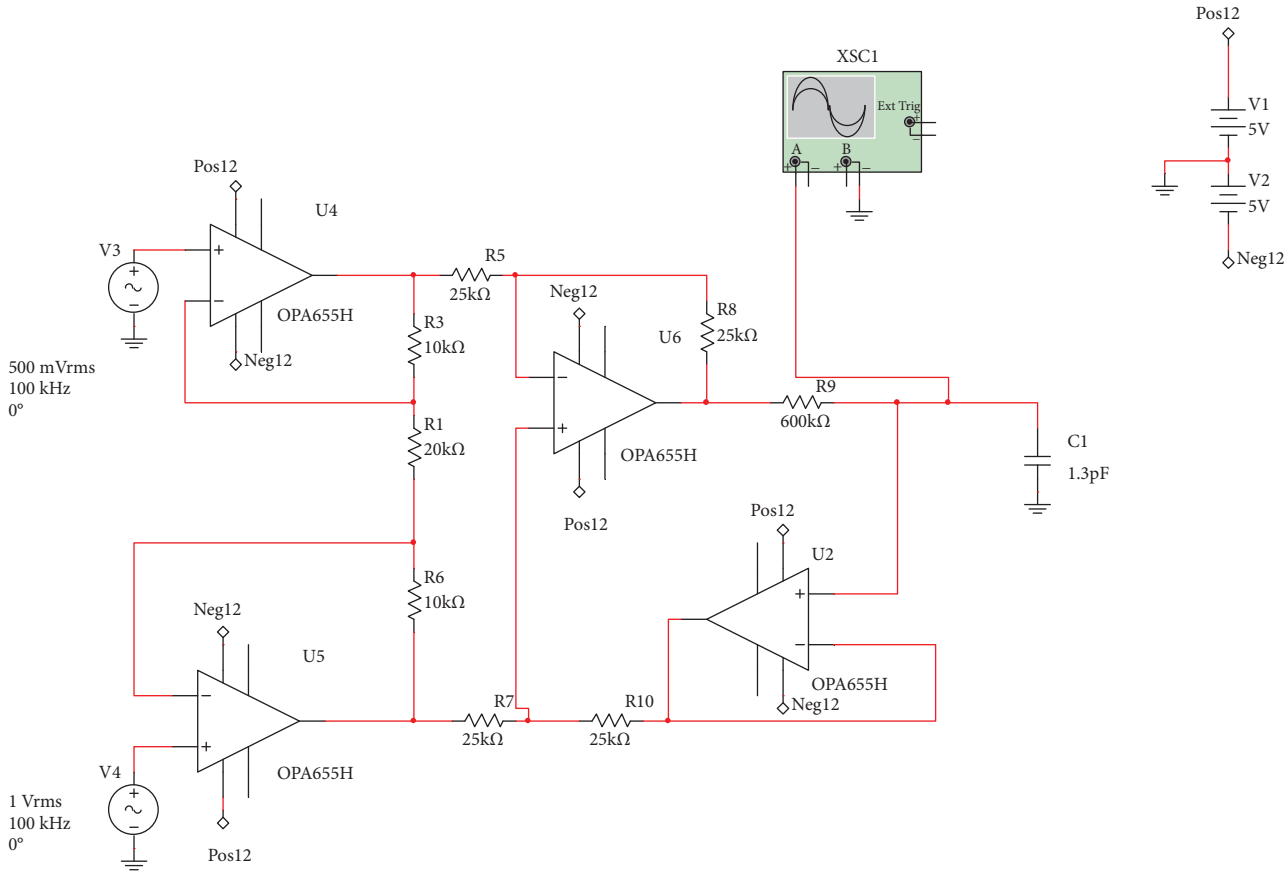

Figure 7: PSPICE simulations.

Moreover, this current must remain constant (signal wave form, amplitude, and RMS value). The current supplied to the probe is given by

$$\bar{I}_{\text{probe}}(jf,D) = \bar{I}_{\text{out}}(jf,D) \times \frac{\bar{Z}_{\text{out}}(jf,D)}{\bar{Z}_{\text{out}}(jf,D)+\bar{Z}_{\text{probe}}(jf,D)},$$
$$\bar{I}_{\text{probe}}(jf,D) = \bar{B}(jf) \times 2\frac{(\bar{V}_1-\bar{V}_2)}{R_{\text{probe}}} \times \frac{\bar{A}(jf)\times R_{\text{probe}}}{\bar{A}(jf)\times R_{\text{probe}}+\bar{Z}_{\text{probe}}(jf,D)}. \quad (12)$$

In order to have a great I_{probe} current, the resistance R_{probe} needs to be small, which implies that the source impedance Z_{out} will decrease and Z_{probe} can no more be overlooked if compared to Z_{out}.

This device must be used in mechanical applications at high rotating speed (such as UGV and turbines). For which it has to operate at a constant frequency of 100 kHz (Equation (13)). When $f < f_0 \Rightarrow \bar{B}(f) = 1$,

$$\bar{I}_{\text{probe}}(jf,D) = 2\frac{(\bar{V}_1-\bar{V}_2)}{R_{\text{probe}}} \times \frac{\bar{A}(jf)\times R_{\text{probe}}}{\bar{A}(jf)\times R_{\text{probe}}+\bar{Z}_{\text{probe}}(jf,D)}. \quad (13)$$

The current modulus supplied to the probe is given by

$$f = 100\text{ kHz} \Rightarrow \begin{cases} I_{\text{out}} = \frac{2}{R_{\text{probe}}}(V_1 - V_2), \\ \bar{Z}_{\text{out}} = \bar{A}(f) \times R_{\text{probe}} = R_{\text{out}} + jX_{\text{out}}, \\ \bar{Z}_{\text{probe}}(D) = -j\frac{1}{2\pi f \varepsilon A_{\text{probe}}} \times D, \\ 1.3\text{ M}\Omega < Z_{\text{probe}}(D) < 2\text{ M}\Omega, \\ K_{\text{probe}} = \frac{1}{2\pi f \varepsilon A_{\text{probe}}} = 32.1\text{ mV}/\mu\text{m} \times \mu A, \end{cases}$$
$$\Rightarrow \bar{I}_{\text{probe}} = \frac{2}{R_{\text{probe}}}(V_1 - V_2) \times \frac{\bar{Z}_{\text{out}}}{R_{\text{out}} + j\left(X_{\text{out}} - K_{\text{probe}} \times D\right)},$$
$$\Rightarrow I_{\text{probe}} = \frac{2}{R_{\text{probe}}}(V_1 - V_2) \times \frac{Z_{\text{out}}}{\sqrt{R_{\text{out}}^2 + \left(X_{\text{out}} - K_{\text{probe}} \times D\right)^2}}. \quad (14)$$

The relative variation of the current supplied to the probe is given by

$$\left(\frac{\Delta I_{\text{probe}}}{I_{\text{probe}}}(D)\right)_{f=100\text{ kHz}} = -K_{\text{probe}} \frac{(X_{\text{out}} - K_{\text{probe}} \times D)}{R_{\text{out}}^2 + (X_{\text{out}} - K_{\text{probe}} \times D)^2} \times \Delta D. \quad (15)$$

The analytical model was validated by the carried out PSPICE simulations (shown in Figure 7).

The IQOA has comparable performances to the other Howland sources. The most important criterion is the choice of the operational amplifiers depending on the desired performances for the source (Table 1). Whatever the choice of the operational amplifiers, the device is not powerful enough to measure the displacements at the nanoscale.

4.2. Design VCCS. To overcome this problem, we designed a voltage-controlled current source, which consists of using two cascaded controllers, a fast but not precise inner control loop tuned by a slow but precise outer control loop used to obtain a high-precision AC (Figure 8) output current. AD9834 circuit is a generator of sinusoidal signals with digital synthesis, which gives it a very high stability in frequency, amplitude, and wave form. The output current is given by Equation (16). This current is converted to voltage V_1 (Equation (17)). As for the voltage, V_2 is generated by the instrumentation amplifier AD620 (Equation (18)).

$$I_{\text{Fullscale}} = I_{\text{FS}} = 18 \times \frac{V_{\text{REF}} - V_{\text{DAC}}}{R_{\text{SET}}}, \tag{16}$$

$$V_1 = rI_{\text{FS}} \times \left(1 + \frac{R_6}{R_7}\right), \tag{17}$$

$$V_2 = G \times R_{\text{probe}} \times I_{\text{probe}}. \tag{18}$$

The current supplied to the probe is given by the following:

$$\begin{aligned}
\bar{I}_{\text{probe}} &= \frac{2}{R_{\text{probe}}}\left(V_1 - \text{GR}_{\text{probe}}\bar{I}_{\text{probe}}\right) \times \frac{\bar{Z}_{\text{out}}}{R_{\text{out}} + j\left(X_{\text{out}} - K_{\text{probe}} \times D\right)}, \\
\bar{I}_{\text{probe}}(D) &= V_1 \times \frac{2}{R_{\text{probe}}} \times \frac{\bar{Z}_{\text{out}}}{R_{\text{out}}\left(1 + 2G + j\left(X_{\text{out}} + 2GX_{\text{out}} - K_{\text{probe}} \times D\right)\right)}, \\
I_{\text{probe}}(D) &= V_1 \times \frac{2}{R_{\text{probe}}} \times \frac{Z_{\text{out}}}{\sqrt{R_{\text{out}}^2(1+2G)^2 + \left(X_{\text{out}}(1+2G) - K_{\text{probe}} \times D\right)^2}}.
\end{aligned} \tag{19}$$

The relative variation of the supplied current to the probe is given by the following:

$$\begin{aligned}
&\left(\frac{\Delta I_{\text{probe}}}{I_{\text{probe}}}(D)\right)_{f=100\,\text{kHz}} \\
&= -K_{\text{probe}} \frac{\left(X_{\text{out}}(1+2G) - K_{\text{probe}} \times D\right)}{R_{\text{out}}^2(1+2G)^2 + \left(X_{\text{out}}(1+2G) - K_{\text{probe}} \times D\right)^2} \times \Delta D
\end{aligned} \tag{20}$$

The performances are given in Table 2.

If we desire high sensitivity, we will need S_{probe}'s value to be big and constant. The supplied current to the probe must be as great and constant as possible regardless of the value of $Z_{\text{probe}(D)}$. The current $I_{\text{probe},max}$ must be less than $I_{\text{probe},max} = V_{CC}/Z_{\text{probe},max}$ so as not to saturate the components.

Table 1: Performances of the source IQOA.

$f = 100$ kHz, $V_1 - V_2 = 500\ mV$				
	$Z_{\text{probe,max}} = 2$ MΩ			
	$R_{\text{probe}} = 100$ kΩ		$R_{\text{probe}} = 600$ kΩ	
Op amp	TL081	OP249	OPA657	OPA655
$\pm V_{\text{CC}}(V)$	± 15	± 15	± 5	± 5
$I_{\text{probe,max}}(\mu\text{A})$	7.5	7.5	2.5	2.5
$I_{\text{probe,max}}(\mu\text{A})$	7.191	7.7	2.332	2.337
$V_{\text{probe,max}}$ (V)	7.9	8.6	4.5	4.476
R_{out}	0.078	0.078	1020	144
X_{out}	1.333	1.56	3.51	47.4
Z_{out}	1.335	1.568	1020	151.26
$\frac{\Delta I}{I}$ (analytical model)	19.7	18.4	0.028	0.14
$\frac{\Delta I_{\text{probe}}}{I_{\text{probe}}}$% (PSPICE)	24	20.5	0.04	0.11

4.3. Discussion of the Simulations Results. The simulation study suggests that only the amplifiers OPA655 and OPA657 can achieve the objective. The current varies depending on the value of the capacitance of the capacitor. AD9834 circuit is a generator of sinusoidal signals with digital synthesis, which gives it a very high stability in frequency, amplitude, and waveform. At the frequency of 100 kHz, K_{probe} is constant. So, the relative uncertainty concerning the sensitivity of the probe is mainly due to variations in the intensity of the current (Equation 22).

According to Equation (6), a variation of the probes voltage amplitude is given by equation (21)

$$\begin{aligned}
\Delta V_{\text{probe}} &= K_{\text{probe}} \times I_{\text{probe}} \times \Delta d_{\text{avg}} \\
&= S_{\text{probe}} \times \Delta d_{\text{avg}}, \\
S_{\text{probe}} &= K_{\text{probe}} \times I_{\text{probe}}.
\end{aligned} \tag{21}$$

Therefore,

$$\frac{\Delta S_{\text{probe}}}{S_{\text{probe}}} \approx \frac{\Delta I_{\text{probe}}}{I_{\text{probe}}}. \tag{22}$$

For the improved quad op-amp current source (IQOA), whatever the choice of the operational amplifiers, the device is not powerful enough to measure the displacements at the nanoscale. Indeed, the relative variation of the current is ≈ 0.04% (for OPA657). With this uncertainty, it is too large to measure the displacements of the order of 10 nm.

For the voltage-controlled current source, the relative uncertainty of the displacements measurement is given by the following (Equation 23)

$$\begin{aligned}
\left(\frac{\Delta\left(\Delta d_{\text{avg}}\right)}{D}\right)_{\text{OPA655}} &= 0.002\% + 0.0148 = 0.0168\%, \\
\left(\frac{\Delta\left(\Delta d_{\text{avg}}\right)}{D}\right)_{\text{OPA657}} &= 0.002\% + 0.0025 = 0.0045\%.
\end{aligned} \tag{23}$$

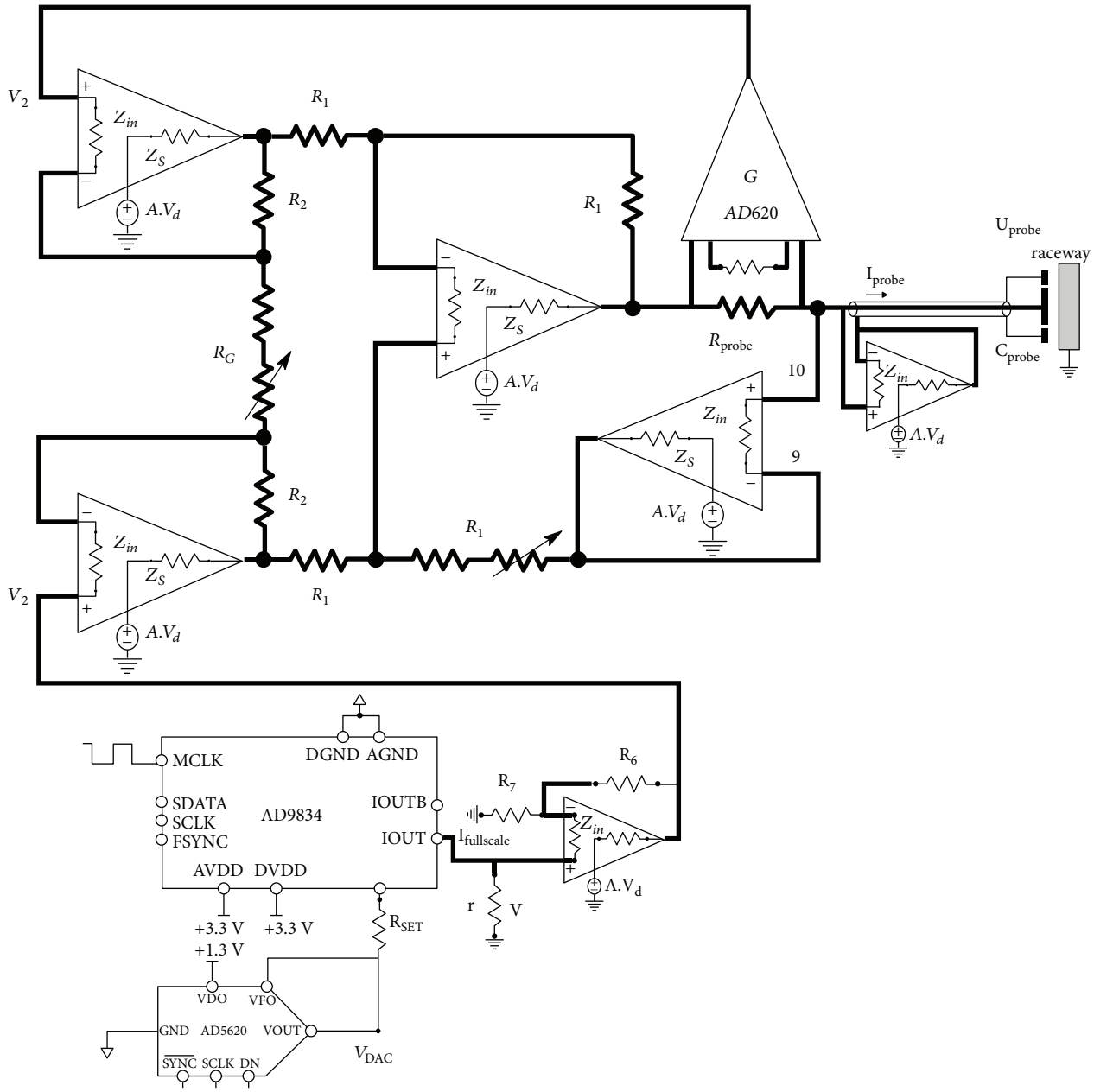

Figure 8: Voltage-controlled current.

The resolution of the device is given by equation 24:

$$\begin{aligned}\Delta\left(\Delta d_{\text{avg}}\right)_{\text{OPA655}} &= 60.10^{3} \times 0.0168\% = 10.08\,\text{nm},\\ \Delta\left(\Delta d_{\text{avg}}\right)_{\text{OPA657}} &= 60.10^{3} \times 0.0045\% = 2.70\,\text{nm}.\end{aligned} \tag{24}$$

The results obtained with the analytical model show that the AC voltage-controlled current source is suitable to measure displacements of the raceway at the nanoscale. Changes in current are reduced despite large variations in capacitive impedances. So, the current can be considered constant and therefore the sensitivity (S_{probe}). Moreover, the carrier frequency allows using this device on the axes of the rotating machines with a high speed.

The stability of this device can be determined from the open-loop transfer function (Equation (25), Figure 9).

$$\begin{aligned}\bar{H}_{\text{OL}}(jf) &= GR_{\text{probe}} \times \frac{2}{R_{\text{probe}}} \times \bar{B}(jf) \\ &\quad \times \frac{\bar{A}(jf) \times R_{\text{probe}}}{\bar{A}(jf) \times R_{\text{probe}} + (1/(jf)) \times (D/(\varepsilon.A_{\text{probe}}2\pi))},\\ \bar{H}_{\text{OL}}(jf) &= GR_{\text{probe}} \times \frac{a^{2}}{(a+2)(a+2)} \\ &\quad \times \frac{(a+1)(a+2) \times R_{\text{probe}}}{(a+1)(a+2) \times R_{\text{probe}} + (1/(jf)) \times (D/(\varepsilon.A_{\text{probe}}2\pi)) \times (3a+2)},\end{aligned} \tag{25}$$

$$\text{Arg}\left(\bar{H}_{\text{OL}}(jf)\right) \geq -90^{\circ} \Rightarrow \text{the device is stable.}$$

Table 2: Performances of the source VCCS.

$f = 100$ kHz				
1.3 MΩ ($D = 0.04$ mm) < Z_{probe} (D) < 2 MΩ ($D = 0.06$ mm)				
	$R_{probe} = 100$ kΩ		$R_{probe} = 600$ kΩ	
	$V_1 = 14.9$ V		$V_1 = 4.9$ V	
Op amp	TL081	OP249	OPA657	OPA655
G	240	240	3	3
$I_{probe,max}$ (μA)	0.145	0.145	2.073	2.073
$V_{probe,max}$ (V)	0.28	0.28	4	4
$\frac{\Delta I_{probe}}{I_{probe}}$ (%)	0.024	0.021	0.0025	0.0148
S_{probe} (mV/μm)	3.32	3.32	47.5	47.5

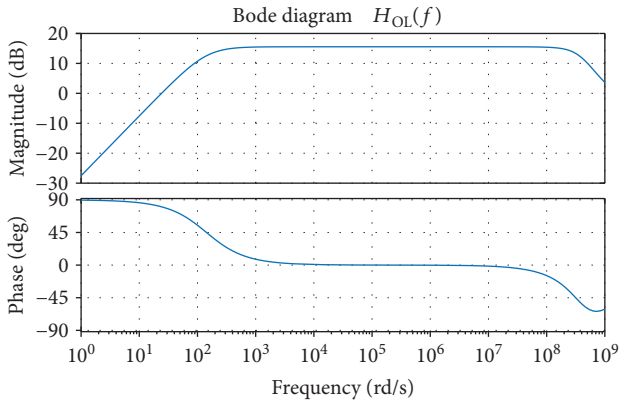

Figure 9: Bode diagram of the open-loop transfer function.

5. Conclusion

In this article, we presented a bearing housing equipped with capacitive probes capable of measuring, in a contactless way, its ring vibration amplitude. All these capacitive probes must be supplied with the same constant current so as to measure the displacement under each probe with the same sensitivity. To measure each displacement at a nanoscale range, the current must be very stable regardless of the values or the variations of the probes impedances. We have shown that the impedance of a Howland current source was not sufficiently large compared with the impedance of a probe and thus the current supplied to the probe varied according to the impedance of that probe, which did not allow us to perform displacements measurements at the nanometer scale. To overcome this problem, we designed a voltage-controlled current source consisting in two nested loops: a fast but imprecise internal control loop tuned by a slow but precise external control loop used to get a stable output of alternating current regardless of the value of the load impedance. The obtained results of the analytical model showed that the performances of the designed device allow the measurement of the bearing rings' vibration amplitude at a nanoscale. Moreover, the bandwidth of this device exceeds the 10 MHz, which made it possible to be used in other applications.

Data Availability

The data used to support the findings of this study are available from the corresponding author upon request.

Conflicts of Interest

The authors declare that they have no conflicts of interest.

Acknowledgments

This work was supported by the Société d'Accélération du Transfert de Technologies (SATT).

References

[1] D. H. Sheingold, "Impedance and admittance transformations using operational amplifiers," *The Lightning Empiricist*, vol. 1, p. 12, 1964.

[2] P. Bertemes-Filho, A. Felipe, and V. Vincence, "High accurate Howland current source: output constraints analysis," *Circuits and Systems*, vol. 4, pp. 451–458, 2013.

[3] P. Bertemes-Filho and A. Felipe, "The effect of the random distribution of electronic components in the output characteristics of the Howland current source," in *XV Int. Conf. on Electrical Bio-Impedance & XIV Conf. on Electrical Impedance Tomography, Journal of Physics: Conference Series*, 2013.

[4] D. Chen and Y. Deng, "Comparison of three current sources for single electrode capacitance measurement," *Review of scientific instrument*, vol. 81, no. 3, article 034704, 2010.

[5] A. Heidari, M. Zanganeh, M. Nahvi, and Nihtianov, "Comparison of three current sources for single electrode capacitance measurement," in *Annual Journal of Electronics, XXII International Scientific Conference*, Sozopol, Bulgaria, 2013.

[6] D. Chen, X. Hu, and W. Yang, "Design of a security screening system with a capacitance sensor matrix operating in single electrode mode," *Measurement Science and Technology*, vol. 22, no. 11, article 114026, 2011.

[7] P. Batra, "A superior current source with improved bandwidth and output impedance for bioimpedance," *Spectroscopy International Journal of Engineering Research and Development* , vol. 12, no. 12, pp. 24–29, 2016.

[8] P. Bertemes-Filho, B. H. Brown, and A. J. Wilson, "A Comparison of modified Howland circuits as current generators with current mirror type circuits," *Physiological Measurement*, vol. 21, no. 1, pp. 1–6, 2000.

[9] Z. Li, X. Zhui, R. Chaoshi, W. Wei, Z. Dechun, and Z. Huiquan, "Study of voltage control current source in electrical impedance tomography system," *Bioinformatics and Biomedical Engineering (iCBBE), 2010 4th International Conference*, vol. 18–20, pp. 1–4, 2010.

[10] M. Zanganeh, "A new high output impedance wideband AC current source with high current swing authority for electrical impedance tomography applications," *International Journal of Computing and Network Technology*, vol. 3, pp. 205–213, 2013.

[11] P. Bertemes-Filho, G. Lima, and H. Tanaka, "An Current source using a negative impedance converter (NIC) for electrical impedance tomography (EIT)," in *17Th International*

Congressof Mechanical Engineering, pp. 10–14, Springer, Cham, São Paulo.

[12] H. Hong, M. Rahal, A. Demosthenous, and R. H. Bayford, "Comparison of a new integrated current source with the modified Howland circuit for EIT applications," *Physiological measurement*, vol. 10, pp. 999, 2009.

[13] A. Ross, G. C. Saulnier, and D. Issacson, "Current source design for electrical impedance tomography," *Physiological Measurement*, vol. 24, pp. 509–516, 2003.

[14] M. Carminati, "Advances in high-resolution microscale impedance sensors," *Journal of Sensors*, vol. 2017, no. Article ID 7638389, p. 15, 2017.

[15] P. Chen, C. Chen, W. Yeh et al., "Using Capacitance sensor to extract characteristic signals of dozing from skin surface," *Journal of Sensors*, vol. 2014, no. Article ID 238350, pp. 1–15, 2014.

[16] M. Neto, R. W. Porto, and J. C. C. Aya, "Design and characterization of a multi-frequency bioimpedance measurement prototype," *First Latin-American Conference on Bioimpedance (CLABIO 2012), Journal of Physics: Conference Series*, vol. 407, p. 2012, 2012.

[17] P. Bertemes-Filho, V. Vincence, M. Santos, and X. Zanatta, "Low power current sources for bioimpedance measurements: a comparison between Howland and OTA-based CMOS circuits," *Journal of Electrical Bioimpedance*, vol. 3, pp. 66–73, 2012.

[18] D. K. Kamat, D. Bagul, and P. M. Patil, "Blood Glucose Measurement Using Bioimpedance Technique," *Advances in Electronics*, vol. 2014, no. Article ID 406257, p. 5, 2014.

[19] R. Nerino, A. Sosso, and G.B. Picotto , "A novel AC current source for capacitance-based displacement measurements," *IEEE Transactions on Instrumentation and Measurement*, vol. 46, no. 2, pp. 640–643, 1997.

[20] S. El-Molla, A. Albrecht, E. Cagatay et al., "Integration of a thin film PDMS-based capacitive sensor for tactile sensing in an electronic skin," *Journal of Sensors*, vol. 2016, no. Article ID 1736169, pp. 1–7, 2016.

[21] T.-H.-N. Dinh, E. Martincic, E. Dufour-Gergam, and P.-Y. Joubert, "Mechanical Characterization of PDMS films for the optimization of polymer based flexible capacitive pressure microsensors," *Journal of Sensors*, vol. 2017, no. Article ID 8235729, pp. 1–9, 2017.

[22] F. Restagno, J. Crassous, E. Charlaix, and M. Monchanin, "A New capacitive sensor for displacement measurement in a surface-force apparatus' measurement," *Science and Technology*, vol. 12, pp. 16–22, 2001.

[23] W. Petchmaneelumka, A. Rerkratn, and A. Kaewpoonsuk, "Digitally programmable AC current source," *Proceedings of the International MultiConference of Engineers and Computer Scientists, Hong Kong, vol. II* , IMECS, 2009.

[24] D. Bouchaala, Q. Shi, and X. Chen, "A High accuracy voltage controlled current source for handheld bioimpedance measurement," in *10Th International Multi-Conferences on Systems, Signals & Devices, 18–21 March*, pp. 18–21, Hammamet, Tunisia, 2013.

[25] F. Seoane, R. Macías, R. Bragós, and K. Lindecrantz, "Simple Voltage-controlled current source for wideband electrical bioimpedance spectroscopy: circuit dependences and limitations," *Measurement Science and Technology*, vol. 22, no. 11, article 115801, 2011.

[26] H. Hong, M. Rahal, and A. Demosthenous, "Floating voltage-controlled current sources for electrical impedance tomography," in *18th European Conference on Circuit Theory and Design, 27–30 Aug.*, pp. 27–30, Seville, Spain, 2007.

[27] A. Azher Al-Obaidi and M. Meribout, "A New enhanced Howland voltage controlled current source circuit for EIT applications," in *IEEE GCC Conference and Exhibition (GCC), 19–22 Feb.*, pp. 19–22, 2011.

[28] Q. Bian, Z. Yan, and Y. Zhao, "Analysis and design of voltage controlled current source for LDO frequency compensation," in *IEEE Conference on Electron Devices and Solid-State Circuits, 19–21 Dec.*, pp. 19–21, Howloon, Hong Kong, 2005.

[29] D. Bouchaala and Q. Shi, "Comparative Study of voltage controlled current sources for biompedance measurements," *International Multi-Conference on Systems, Sygnals & Devices, 20–23 March*, pp. 20–23, 2012.

[30] P. Marconnet, B. Pottier, L. Rasolofondraibe, and J.P. Dron, "Measuring load distribution on the outer raceways for rotating machines," *Mechanical Systems and Signal processing, MSSP*, vol. 66-67, no. 2016, pp. 582–596, 2015.

[31] L. Rasolofondraibe, B. Pottier, P. Marconnet, and E. Perrin, "Numerical model of the capacitive probe's capacitance for measuring the external loads transmitted by bearing's rolling elements of rotating machines," *IEEE Sensor Journal*, vol. 13, no. 8, pp. 3067–3072, 2013.